Three-level filter for increased depth of focus and Bessel beam generation

Colin JR Sheppard[1, 3*] and Shalin Mehta[2, 3]

[1]*Italian Institute of Technology, Via Morego 30, Genova 16163, Italy*
[2]*Cellular Dynamics Program, Marine Biological Laboratory,7 MBL Street, Woods Hole, Massachusetts 02543, USA*
[3]*Singapore-MIT Alliance for Research and Technology (SMART) Centre, 3 Science Drive 2, Singapore 117543, Singapore*
**colinjrsheppard@gmail.com*

Abstract: A novel axially-symmetric filter for increasing focal depth and generating an approximation to a Bessel beam is proposed. It consists of an array of rings of strength –1,0 and 1. The design is based on an analytic solution, and combines high resolution in the transverse direction with good efficiency. One presented design increases the depth of focus compared with a standard lens by more than 30 times, with a very flat axial intensity distribution over this range. Effects of discretization are discussed. Various different approaches to increasing depth of focus are compared, to put the new design into perspective.

OCIS Codes: (050.1220) Apertures; (050.1940) Diffraction; (070.2580) Paraxial wave optics; (110.6980) Transforms; (350.6980) Transforms.

References and links

1. M. Mazilu, D. J. Stevenson, F. Gunn-Moore, and K. Dholakia, "Light beats the spread: "non-diffracting" beams," Laser Photon. Rev. **4**(4), 529–547 (2010).
2. J. H. McLeod, "The axicon: A new type of optical element," J. Opt. Soc. Am. **44**(8), 592–597 (1954).
3. J. Dyson, "Circular and spiral diffraction gratings," Proc. R. Soc. Lond. A Math. Phys. Sci. **248**(1252), 93–106 (1958).
4. G. B. Airy, "The diffraction of an annular aperture," Phil. Mag. Ser. 3 **18**, 1–10 (1841).
5. J. W. S. Rayleigh, "On the diffraction of object glasses," Mon. Not. R. Astron. Soc. **33**, 59–63 (1872).
6. G. C. Steward, "IV Aberration diffraction effects," Phil. Trans. Roy. Soc. London Ser. A **225**(626-635), 131–198 (1926).
7. E. H. Linfoot and E. Wolf, "Diffraction images in systems with an annular aperture," Proc. Phys. Soc. B **66**(2), 145–149 (1953).
8. B. J. Thompson, "Diffraction by semitransparent and phase annuli," J. Opt. Soc. Am. **55**(2), 145–149 (1965).
9. G. Yang, "An optical pickup using a diffractive optical element for a high-density optical disc," Opt. Commun. **159**(1-3), 19–22 (1999).
10. H. F. Wang and F. Gan, "High focal depth with a pure-phase apodizer," Appl. Opt. **40**(31), 5658–5662 (2001).
11. E. R. Dowski, Jr. and W. T. Cathey, "Extended depth of field through wave-front coding," Appl. Opt. **34**(11), 1859–1866 (1995).
12. C. J. R. Sheppard and T. Wilson, "Gaussian-beam theory of lenses with annular aperture," IEE J. Microwaves Opt. Acoust. **2**(4), 105–112 (1978).
13. J. Durnin, "Exact solutions for nondiffracting beams. I. the scalar theory," J. Opt. Soc. Am. A **4**(4), 651–654 (1987).
14. C. J. R. Sheppard, "Binary phase filters with a maximally-flat response," Opt. Lett. **36**(8), 1386–1388 (2011).
15. C. J. R. Sheppard, J. Campos, J. C. Escalera, and S. Ledesma, "Three-zone pupil filters," Opt. Commun. **281**(14), 3623–3630 (2008).
16. F. Gori, G. Guattari, and C. Padovani, "Bessel-Gauss beams," Opt. Commun. **64**(6), 491–495 (1987).
17. A. J. Cox and J. D'Anna, "Constant-axial-intensity nondiffracting beam," Opt. Lett. **17**(4), 232–234 (1992).
18. M. V. Berry and N. L. Balazs, "Nonspreading wave packets," Am. J. Phys. **47**(3), 264–267 (1979).
19. G. A. Siviloglou, J. Broky, A. Dogariu, and D. N. Christodoulides, "Observation of accelerating Airy beams," Phys. Rev. Lett. **99**(21), 213901 (2007).
20. M. R. Arnison, C. J. Cogswell, C. J. R. Sheppard, and P. Török, "Wavefront coding fluorescence microscopy using high aperture lenses," in *Optical Imaging and Microscopy* P. Török and F.-J. Kao, eds. (Springer, 2003), pp. 143–168.
21. R. Boivin and A. Boivin, "Optimized amplitude filtering for superresolution over a restricted field - I. Achievement of maximum central irradiance under an energy constraint," Opt. Acta (Lond.) **27**, 857 (1980).
22. C. J. R. Sheppard and Z. S. Hegedus, "Axial behaviour of pupil plane filters," J. Opt. Soc. Am. A **5**(5), 643–647 (1988).

#172811 - $15.00 USD Received 17 Jul 2012; revised 23 Aug 2012; accepted 23 Aug 2012; published 19 Nov 2012

23. Y. S. Xu, J. Singh, C. J. R. Sheppard, and N. G. Chen, "Ultra long high resolution beam by multi-zone rotationally symmetrical complex pupil filter," Opt. Express **15**(10), 6409–6413 (2007).
24. V. F. Canales, J. E. Oti, and M. P. Cagigal, "Three-dimensional control of the focal light intensity distribution by analytically designed phase masks," Opt. Commun. **247**(1-3), 11–18 (2005).
25. Z. Bouchal, J. Wagner, and M. Olivik, "Bessel beams in the focal region," Opt. Eng. **34**(6), 1680–1688 (1995).
26. Y. Kozawa and S. Sato, "Sharper focal spot formed by higher-order radially polarized laser beams," J. Opt. Soc. Am. A **24**(6), 1793–1798 (2007).
27. Y. Kozawa, T. Hibi, A. Sato, H. Horanai, M. Kurihara, N. Hashimoto, H. Yokoyama, T. Nemoto, and S. Sato, "Lateral resolution enhancement of laser scanning microscopy by a higher-order radially polarized mode beam," Opt. Express **19**(17), 15947–15954 (2011).
28. C. J. R. Sheppard, "Synthesis of filters for specified axial properties," J. Mod. Opt. **43**(3), 525–536 (1996).
29. M. R. Foreman, S. S. Sherif, P. R. T. Munro, and P. Török, "Inversion of the Debye-Wolf diffraction integral using an eigenfunction representation of the electric fields in the focal region," Opt. Express **16**(7), 4901–4917 (2008).
30. T. Čižmár and K. Dholakia, "Tunable Bessel light modes: engineering the axial propagation," Opt. Express **17**(18), 15558–15570 (2009).
31. J. Wang, W. Chen, and Q. W. Zhan, "Engineering of high purity ultra-long optical needle field through reversing the electric dipole array radiation," Opt. Express **18**(21), 21965–21972 (2010).
32. H. F. Wang, L. Shi, B. Luk`yanchuk, C. Sheppard, and C. T. Chong, "Creation of a needle of longitudinally polarized light in vacuum using binary optics," Nat. Photonics **2**(8), 501–505 (2008).
33. C. J. R. Sheppard, S. Rehman, N. K. Balla, E. Y. S. Yew, and T. W. Teng, "Bessel beams: Effects of polarization," Opt. Commun. **282**(24), 4647–4656 (2009).
34. X. Hao, C. F. Kuang, T. T. Wang, and X. Liu, "Phase encoding for sharper focus of the azimuthally polarized beam," Opt. Lett. **35**(23), 3928–3930 (2010).
35. C. J. R. Sheppard and S. Rehman, "Highly convergent focusing of light based on rotating dipole polarization," Appl. Opt. **50**(22), 4463–4467 (2011).

1. Introduction

Numerous papers recently have been concerned about ways to improve depth of focus, while maintaining good transverse resolution and efficiency [1]. There are several different approaches, most of which were introduced many years ago, including the following:

- axicon [2],
- diffractive axicon [3],
- annular aperture [4–7],
- binary phase array of annuli [8–10],
- cubic phase mask [11].

The refractive axicon can give very long focal depth, but is in essence a macroscopic device based on geometric optics, which can produce strong intensity fluctuations along the optical axis. The diffractive axicon is like a Fresnel lens but with constant ring widths, and has similar limitations to the refractive type. An annular aperture, used with a lens, produces an axial intensity that is stretched out without change of shape, accompanied by a sharpening of the focal spot. In the limiting case of a narrow annulus, the focal depth tends to infinity and a Bessel beam is produced [6, 12, 13]. This is accompanied by a huge loss in power, but this problem can be overcome by combining with illumination using an axicon. Alignment is not severe if the annulus is not too narrow. A practical limit to the achievable DoF is set by diffraction by the annular aperture.

Binary arrays of phase annuli can produce an improvement in depth of focus (DoF) that increases with the number of rings. Recently a strategy was described for analytically designing a binary array with a flat axial response, giving a maximally-flat (MF) filter [14]. The design principle is that low-order derivatives of the axial intensity around the focal plane are set to zero by choice of the same number of array element boundaries. The pth derivative of the axial amplitude is proportional to the pth moment of the pupil. By choosing $n-1$ boundaries causing the lowest order moments of the binary pupil to be zero, we designed analytically pupils that give rise to an axial intensity whose first $2n-1$ derivatives around the focal plane are zero. For an array of five rings of alternating sign, the distance along the axis

#172811 - $15.00 USD Received 17 Jul 2012; revised 23 Aug 2012; accepted 23 Aug 2012; published 19 Nov 2012

between the points where the intensity drops to 90% is increased by a factor of 8.3 compared with a circular pupil, although there is some accompanying loss of power (Strehl ratio is 13%) [14]. The intensity in a meridional plane using such filters is shown in Fig. 1, where it is compared with the result for a circular pupil. A more modest improvement of 4.6 times is achieved with three rings [10, 15]. These filters give good approximation to a Bessel beam over a finite propagation distance. They result in finite energy beams that give much more uniform axial intensity than Bessel-Gauss beams [12, 16], or some other approximations to a Bessel beam [17]. They are also generated from a finite pupil, unlike Bessel-Gauss beams. Potential applications include optical coherence tomography, and confocal, multiphoton and scanned light sheet microscopy.

The cubic phase mask can give a large increase in DoF: an increase of 30 times has been described [11]. This is usually used in combination with digital restoration, as the raw point-spread function is blurred. For this reason, the overall noise behavior is difficult to compare with the other methods, but the Strehl ratio at the focus is only about 0.1%. The cubic phase mask is non-axially symmetric, unlike the other methods considered here. This may be a disadvantage for some applications, but an advantage is the achromatic property. The cubic phase mask is closely related to the Airy beam [18]. Although it has been reported that the first observation of Airy beams was made only in 2007 [19], effectively an approximation to an Airy beam is observed in cubic phase imaging experiments. For example, Arnison *et al.* experimentally observed the point spread function in a fluorescence microscope with a cubic phase mask [20].

It is often claimed that phase masks are superior to amplitude masks as the latter absorb energy. However, in some applications the energy throughput is not the most important factor: the relative strength of the side lobes can be more important [21, 22]. In this case the annular pupil, as an example of an amplitude mask, can be superior compared with other approaches. And, for focusing radiation as in a confocal microscope, as already mentioned, an axicon can be used for illumination of the annular mask, and loss of energy is no longer a problem. Amplitude masks can give good performance, as they can reduce the relative side lobe strength compared with that using a phase mask. Xu *et al.* described a mixed amplitude/phase mask consisting of rings with amplitude strengths –1, 0 and 1 [23]. An increase in DoF of 16 times was achieved using a 7-ring mask. The mask gives a Strehl ratio of 1.8%. The principle behind the performance of this filter was not discussed. It might be thought that the mechanism is that the zero strength rings provide a more gradual variation from –1 to 1, but analysis seems to show that this is not the case. Rather, the filter is basically a 2-ring MF element to flatten the axial response, combined with a central obscuration, as in an annular aperture, to stretch it further. A few more elements were used to tune the overall behavior. This observation suggests that interesting filter designs could result from combining MF elements with a central obscuration. The strategy is that the axial intensity is flattened by the MF elements and stretched further by the annular shape, resulting in an increased DoF.

This procedure should be preferable to increasing the number of MF elements. Although in principle the number can be increased to obtain unlimited depth of field, in practice we could not solve numerically the simultaneous equations for more than 6 elements. The dimensional tolerances also become severe for many elements.

2. Comparison of existing designs

First we compare performance of some of the existing designs for scalar, paraxial focusing. As in previous work we define the parameters *S*, *F* and *G* [22]. The filter amplitude transmittance is given by $Q(t)$, assumed real with maximum value $Q_{\max}$, where

#172811 - $15.00 USD Received 17 Jul 2012; revised 23 Aug 2012; accepted 23 Aug 2012; published 19 Nov 2012

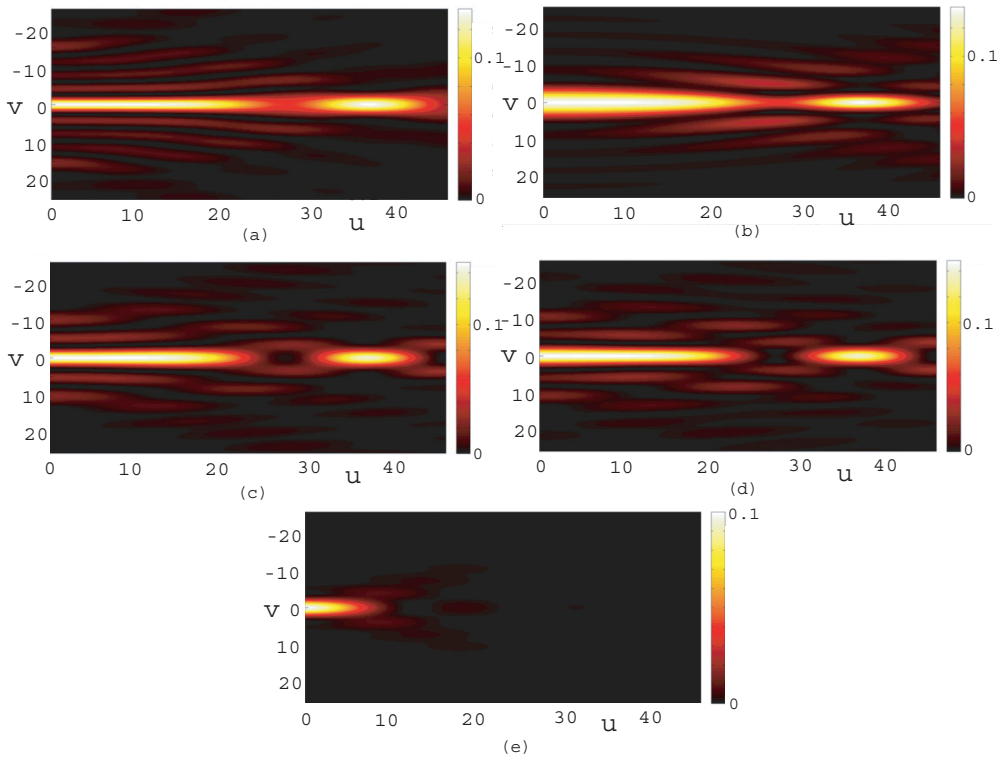

Fig. 1. The intensity in a meridional plane for: (a) – (d) the four different solutions for a maximally-flat pupil (MF) of 5 elements, (e) a circular pupil, calculated using fast Fourier transform with a sampling distance of 0.004 of the pupil radius. Solution (a) gives the smallest focal spot. Pairs of solutions (a), (b) and (c), (d) each give the same axial intensity.

$t = \rho^2, 0 < t < 1$ and ρ is the normalized pupil radius. Then S is the intensity at the focus, given by $S = q_0^2 / |Q_{\max}|^2$, where the pth moment of the pupil is defined by

$$q_p = \int_0^1 Q(t)\, t^p dt. \tag{1}$$

F is the normalized ratio of the intensity at the focus to the focused energy, and is given by

$$F = \frac{q_0^2}{\int_0^1 |Q(t)|^2 dt}. \tag{2}$$

G is called the transverse gain factor, which is equal to the square of the normalized parabolic width of the intensity point spread function, and is given by

$$G = \frac{2q_1}{q_0}. \tag{3}$$

S, F and G are all unity for a plain circular pupil. For an annular pupil with normalized inner radius ρ_0, we have $q_0 = 1 - \rho_0^2$, $q_1 = (1 - \rho_0^4)/2$, and $Q_{\max} = 1$, and so $S = F^2 = (2 - G)^2$. For the limiting case of an annular pupil of infinitesimal thickness, $G = 2$.

#172811 - $15.00 USD Received 17 Jul 2012; revised 23 Aug 2012; accepted 23 Aug 2012; published 19 Nov 2012

Figure 2(a) compares the behavior of S versus G for an annular pupil, a 2-ring binary phase filter (levels ± 1), and MF filters with 2-5 rings. We observe that the value of S for a given G is highest for the 2-ring binary phase filters [24]. The MF filters give higher S than for the annulus, but lower (except for 2 rings) than for the 2-ring binary filter. Also shown is the behavior of F for the annular pupil. It is seen that if F is the important parameter, then the annular pupil performs better than the binary filters. Figure 2(b) shows the variation of G with the DoF, defined by the parameter W_{90}, the normalized axial distance between the points where the intensity drops to 90% of the peak value. For an annular pupil, the shape of the axial intensity variation is independent of the obscuration, and $W_{90} = 1/F = S^{-1/2}$. The MF filters give greater W_{90} for a given G compared with an annular pupil. Note that binary phase filters could be designed to give a further improved W_{90}, compared with MF filters, by allowing small axial variations in intensity. Figure 2(c) shows the variation of S and F with W_{90}. MF exhibits better S and F than the annular pupil, and at the same time the axial intensity is much flatter.

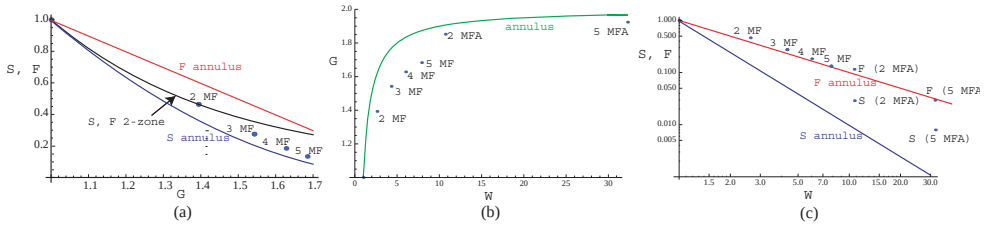

Fig. 2. Parameters for different strategies to achieve increased depth of focus. (a) The parameters S and F as functions of G, the transverse gain, for an annular pupil, 2-zone binary phase filters, and maximally-flat (MF) filters of 2-5 elements. (b) The parameter G plotted against W_{90}, the 90% depth of focus. MF and MFA solutions are compared with an annular pupil. (c) The parameters S and F as functions of W_{90} for MF filters, MFA filters, and annular pupils.

3. A three level filter

We now consider the combination of MF elements with a central obscuration. We call these MFA (maximally-flat annulus) filters. In general the amplitude in the focal region for a mask $Q(t)$ can be written [22]

$$U(v,u) = \int_0^1 Q(t) J_0(v\sqrt{t}) \exp(-iut/2) dt, \qquad (4)$$

where $v = 2\pi kr \sin\alpha$ and $u = 4kz \sin^2(\alpha/2)$ are optical coordinates related to cylindrical coordinates r, z in the focal region, $k = 2\pi/\lambda$, and α is the angular semi-aperture of the lens. The axial amplitude ($v = 0$) is shown from Eq. (4) to be the Fourier transform of $Q(t)$. This means that by making a central obscuration of width t_0 simply scales linearly the axial intensity given by the rest of the filter. A typical value for t_0 might be 3/4 (i.e. $\rho_0 = \sqrt{3}/2 = 0.866$), which for a plain annulus would give $W_{90} = 4$, $G = 7/4$, $S = 1/16$, $F = 1/4$ (see Table 1), so that (unless illuminated by an axicon) 25% of the power is transmitted. To obtain MFA filters from previously designed MF filters, the boundaries between regions are scaled linearly in t, and so should be set at $\rho_{i\mathrm{MFA}} = [t_0 + (1-t_0)t_i]^{1/2}$, where t_i are the values for the unobstructed case [14]. Then

#172811 - $15.00 USD Received 17 Jul 2012; revised 23 Aug 2012; accepted 23 Aug 2012; published 19 Nov 2012

$W_{90\mathrm{MFA}} = W_{90}/(1-t_0)$, $G_{\mathrm{MFA}} = [2t_0 + G(1-t_0)]$, $S_{\mathrm{MFA}} = (1-t_0)^2 S$, and $F_{\mathrm{MFA}} = (1-t_0)S$, in each case the value of the parameter with subscript MFA (A standing for annulus) being given in terms of the corresponding MF values without subscript. G is close to 2, the value corresponding to a Bessel beam. As an example, for a 5-ring MF element (first solution) with $t_0 = 3/4$ (i.e. a total of 6 elements), $W_{90} = 33$, $G = 1.92$, $S = 0.8\%$ and $F = 0.03$. These, and other cases, are given in Table 1, and the parameters also plotted in Fig. 2(b) and 2(c). The MFA solutions give higher values of S than a plain annulus. The values of F are similar, as the beam is close to a Bessel beam. The intensities along the axis and in the focal plane for the 5-ring and 2-ring cases are shown in Fig. 3. The axial response for both 5-ring and 2-ring cases is very flat, and the transverse intensity similar to a Bessel beam. The axial intensity is much more uniform than using an annulus alone, and the efficiency also higher. Although we compute the filter boundaries analytically as described above, the intensity distribution in the focal region is simulated in Fig. 4 on a discrete grid. The discrete simulation allows us to evaluate the sensitivity to discretization when the pupils are implemented with discrete devices, such as a spatial light modulator (SLM). All filter responses in Figs. 1 and 4 are computed by the fast Fourier transform algorithm with a sampling distance of 0.004 in normalized pupil coordinates. The normalized sampling distance of 0.004 corresponds to 500 samples over the normalized diameter ($=2$) of the pupil, which can be easily implemented with current generation SLMs that typically provide 800×600 pixels or more.

Table 1. Performance Parameters for Different Filter Strategies

	W_{90}	***G***	***S***	***F***
Circular	1	1.0	1.0	1.0
MF3	4.6	1.54	0.275	0.275
MF5	8.3	1.68	0.133	0.133
Annulus	4	1.75	0.063	0.25
($t_0 = 0.75$)				
Annulus	10	1.9	0.01	0.1
($t_0 = 0.9$)				
Annulus	33.3	1.97	0.0009	0.03
($t_0 = 0.97$)				
Bessel beam	∞	2.0	0	0
MFA2	11.2	1.85	0.029	0.116
MFA5	33.2	1.92	0.008	0.03
F10	21	1.81	0.047	0.047
F10A	84	1.95	0.003	0.012

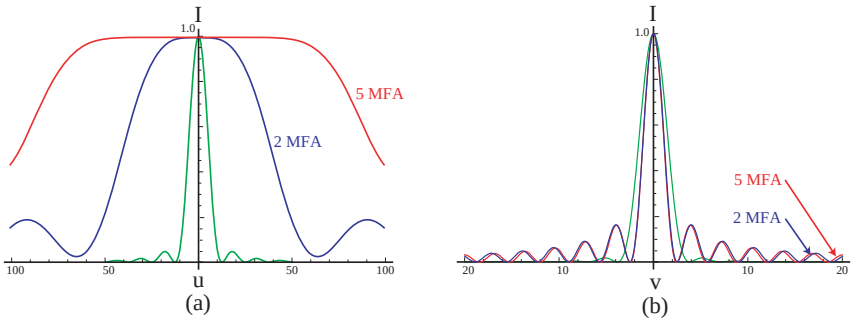

Fig. 3. The intensity in the focal region for MFA pupils of 2 and 5 elements (total 3 or 6 rings). (Solution (a) for 5 elements.) (a) Axial intensity. (b) Transverse intensity. The behavior for a circular aperture is shown in green for comparison.

For the MF filters described previously [14], for 5 rings there are four possible solutions, as shown in Fig. 1. There are two different axial intensity distributions, and two filter solutions for each of them, mirror images of each other in coordinate t. The solution

#172811 - $15.00 USD Received 17 Jul 2012; revised 23 Aug 2012; accepted 23 Aug 2012; published 19 Nov 2012

illustrated in Fig. 1(a) is the one that gives the smallest focal spot. The other solution with the same axial response exhibits the broadest focal spot of the four (Fig. 1(b)). The remaining two solutions are shown in Figs. 1(c) and 1(d). For the MFA filters, again there are four solutions for 5-ring MFA (with a total of 6 elements including the central obscuration), as shown in Fig. 4(a)–4(d). For MFA, the focal spot size for the four solutions is similar.

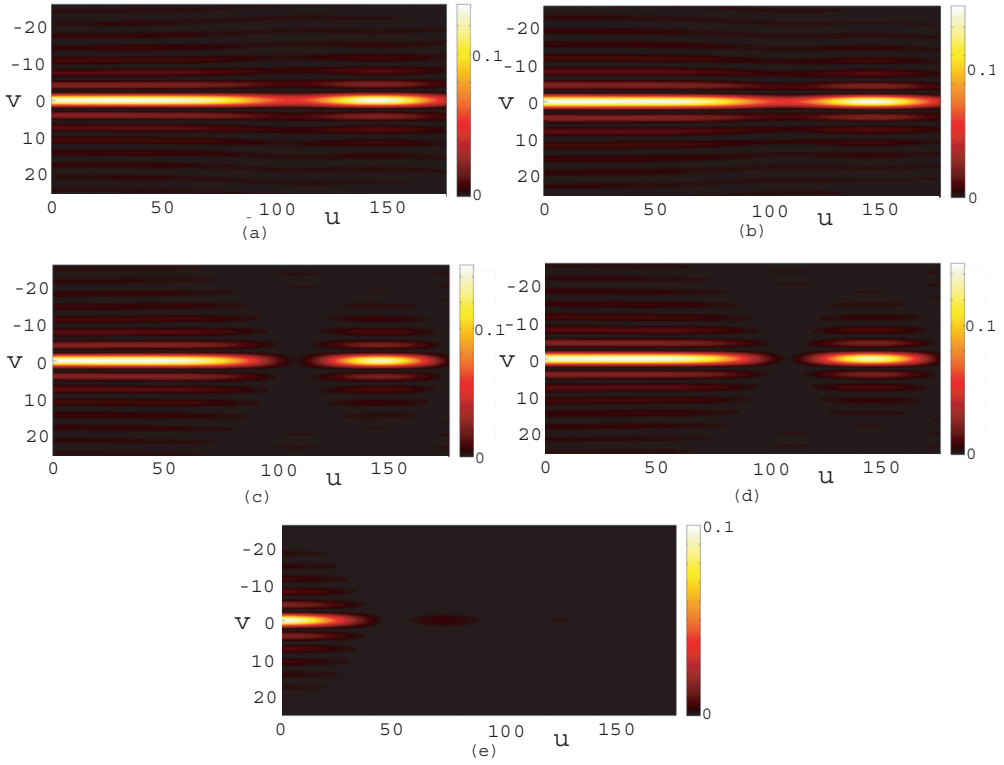

Fig. 4. The intensity in a meridional plane for (a-d) the four solutions for an annular maximally-flat pupil (MFA) of 5 elements (total 6 rings) ($t_0 = 0.75$), (e) a plain annular pupil ($t_0 = 0.75$). These are calculated using fast Fourier transform with a sampling distance of 0.004 of the pupil radius. Solution (a) gives the smallest focal spot, but all solutions give close to a Bessel beam in the transverse direction. Pairs of solutions (a), (b) and (c), (d) each give the same axial intensity. Note the different axial scale from Fig. 1.

4. Sensitivity to errors and pixelation

We investigated the sensitivity of the MF filters to errors in ring radius. Figure 5 shows the effect on the axial intensity when using radii truncated to 3, 2, 1.5 (i.e. with second decimal place 0 or 5) and 1 decimal places, respectively. The actual values taken for the radii are {1, 0.716, 0.544, 0.367, 0.185, 0}, {1, 0.71, 0.54, 0.37, 0.19, 0}, {1, 0.70, 0.55, 0.40, 0.20, 0}, {1, 0.7, 0.5, 0.3, 0.2, 0}. These correspond to solution (a) for 5 elements. It is seen that 2 decimal places gives a flat response, although the depth of field is decreased relative to the more accurate result. If the rings are written using a pixelated device such as an SLM, rather than using an axially symmetric structure, we might expect the errors to be more important. Figures 6, 7 show the pixilated filters used for the simulations presented in Figs. 1, 4, corresponding to 500×500 pixels. The pixelation is very obvious in the filter transmission, and some of the rings are very narrow for the MFA filters. However, transverse and axial intensity plots for these filters are shown in Fig. 8, demonstrating that they are quite robust.

#172811 - $15.00 USD Received 17 Jul 2012; revised 23 Aug 2012; accepted 23 Aug 2012; published 19 Nov 2012

The pixelation was performed automatically, and we expect some improvement could be obtained by further optimization.

5. Further observations

Investigation of the element radii for the family of MF solution (a) (with greatest G) shows that the radii are close to proportional to the integers, except for the outer ring. For example, for 5 elements we have as a starting design {0, 0.2, 0.4, 0.6, 0.8, 1}, and by evaluating the axial intensity we find the performance is improved by changing the outer radius: {0, 0.2, 0.4, 0.6, 0.8, 1.1135}. Then renormalizing and approximating, we obtain {0, 0.18, 0.36, 0.54, 0.72,

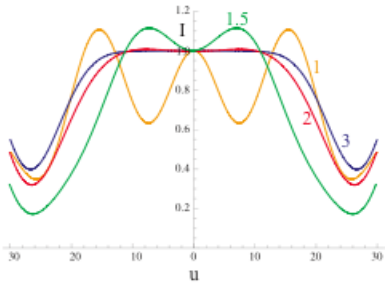

Fig. 5. The axial intensity for five element MF filters, with ring radii truncated to 3, 2, 1.5 and 1 decimal place.

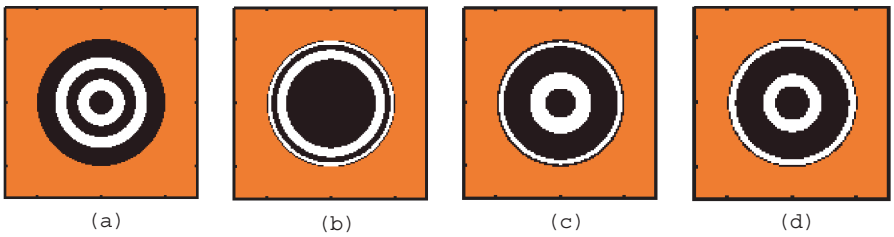

Fig. 6. The pixelated filters used in our simulations for MF filters. The four solutions for five elements are shown.

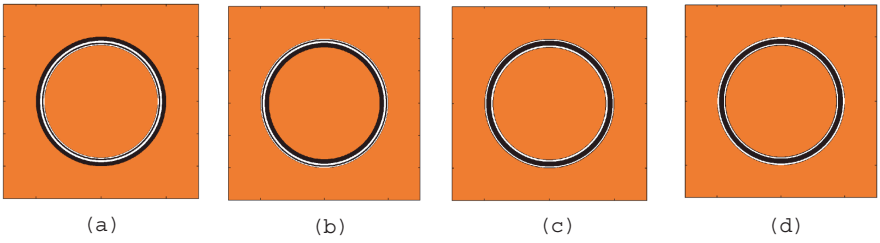

Fig. 7. The pixelated filters used in our simulations for MFA filters. The four solutions for five elements are shown.

1}, giving $W_{90} \approx 5$. This compares with the exact design (to 5 decimal places) {0, 0.18512, 0.36726, 0.54412, 0.71610, 1}, giving $W_{90} \approx 8.3$. In this way we can generate designs for larger number of elements. For example, for a 10-element filter with uniform spacing except for the largest ring, {0, 0.093, 0.186, 0.279, 0.371, 0.464, 0.557, 0.645, 0.743, 0.836,1}, we have $W_{90} \approx 18$. This could be used as a starting point for further optimization. Fitting the ring

#172811 - $15.00 USD Received 17 Jul 2012; revised 23 Aug 2012; accepted 23 Aug 2012; published 19 Nov 2012

radii to a cubic gives the filter {0, 0.100, 0.196, 0.290, 0.384, 0.477, 0.570, 0.661, 0.751, 0.841,1}, which further improves the flatness of the axial intensity, and gives $W_{90} \approx 21$. Constructing an annular filter with $\rho_0 = 0.866$ as before would then give $W_{90} \approx 84$. Some properties of these last two cases are also given in Table 1 and Fig. 2, as F10 and F10A.

An array of equal width elements gives the well-known design for a diffractive axicon [3]. Combined with a lens it produces a double-ring focus. So now we can see an explanation of the mechanism of operation for the family of MF filters giving greatest *G*: the diffractive axicon diffracts the light away from the focal region to produce a central shadow, while the excess part of the outer ring produces a Bessel-like beam in the interior shadow region, which interferes with the side-lobes of the double-ring structure. As the number of elements increases, the focal field tends towards that of a Bessel beam. This is similar to the mechanism of focusing from a truncated Bessel J_0 pupil [25], which also has elements of approximately equal width, apart from the truncated element. For our solution with lowest *G*, the excess is at the center of the pupil, and so the beam becomes larger as the number of elements increases. For our other solutions, the excess is in an intermediate zone of the pupil. Kozawa and associates have reported using a filter to give improved transverse resolution, and also presented impressive experimental results with a confocal system [26, 27]. Their filter also consists of 5 rings of close to equal width, with an outer ring of a different width. Their experimental result shows an increase in depth of focus, illustrating that the point spread

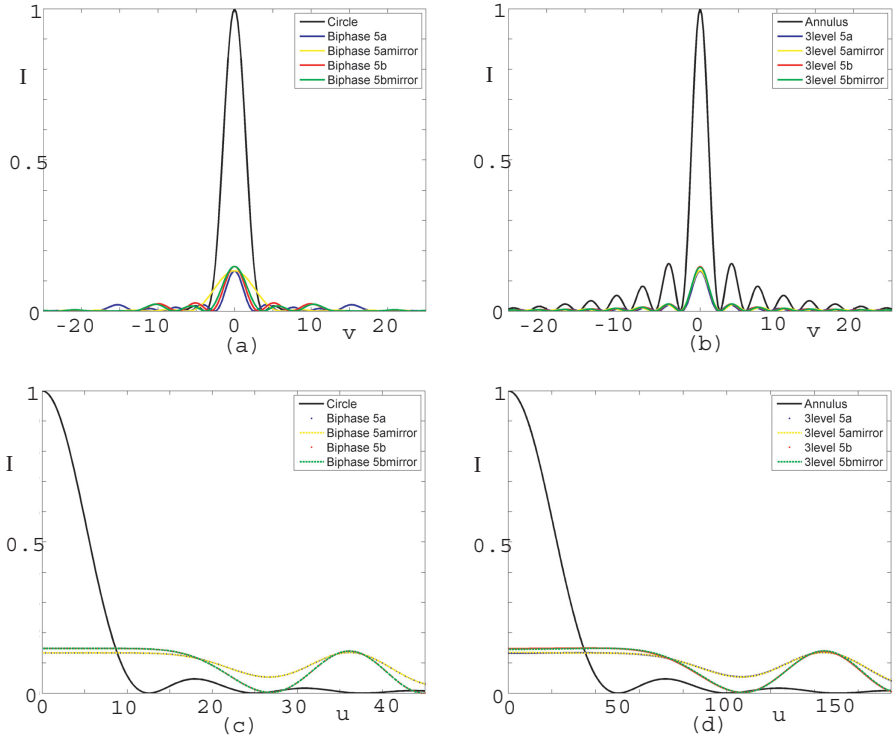

Fig. 8. The transverse (a), (b) and axial (c), (d) intensities (un-normalized) for: (a), (c) pixelated 5 ring MF (labeled biphase), and (b), (d) pixilated MFA filters (labeled 3 level). Results for a circular pupil and an annular pupil are also shown. 5a and 5b correspond to the two different axial intensity variations, while 5amirror, 5bmirror correspond to the filters that are mirror images in coordinate *t* of 5a and 5b.

#172811 - $15.00 USD Received 17 Jul 2012; revised 23 Aug 2012; accepted 23 Aug 2012; published 19 Nov 2012

function is close to a Bessel beam. They explain the operation of their filter in terms of a higher order Laguerre-Gauss mode, with a scale optimized relative to the pupil radius, but as the zeros of the Laguerre polynomial are also approximately equally spaced in radius, the connection with the Laguerre mode may be fortuitous.

6. Conclusions

A novel design for pupil masks to give greatly increased depth of focus has been presented. The method is based on arrays of rings of amplitude strengths –1, 0 and 1. A 30 times increase results with one of the designs. The transverse spot size is also reduced. The approach can be used to generate an approximation to a Bessel beam. It also sheds some light on the mode of operation of previously presented filter designs. The mask could be manufactured using thin film technology, or our simulations show it could be generated using 512×512 pixel liquid crystal modulators. Although several methods for designing pupil masks to increase focal depth have been presented [28–31], many of them give axial intensity distributions that exhibit pronounced ripple, whereas the present design is exceedingly flat.

In order to stress the general principle, the design here is based on the scalar paraxial approximation, based on an analytic solution rather than an optimization. Our previous experience suggests that it could be readily adapted to high numerical aperture focusing, using different polarization distributions. In particular, it could be combined with radially-polarized illumination, or azimuthally-polarized illumination with a vortex, to produce a needle of longitudinally polarized light [32] or circularly polarized light [33–35], respectively. The present design gives a depth of focus increase of a factor of over 30 (to give 15λ for 0.95 NA), as compared with about a factor of 8 (4λ for 0.95 NA) in Ref. 29.

Acknowledgment

Support from the Singapore-MIT Alliance for Research and Technology (SMART) Program is acknowledged. SM acknowledges a post-doctoral fellowship from Human Frontier Science Program (HFSP).

#172811 - $15.00 USD Received 17 Jul 2012; revised 23 Aug 2012; accepted 23 Aug 2012; published 19 Nov 2012